

# A CONTRAST EFFICIENCY FUNCTION FOR QUANTITATIVELY MEASURING THE SPATIAL-RESOLUTION CHARACTERISTICS OF SCANNING SYSTEMS

F. D. Rollo and A. G. Schulz

*The Johns Hopkins Medical Institutions, Baltimore, Maryland  
and the Johns Hopkins University Applied Physics Laboratory, Silver Spring, Maryland*

At the present stage of development of imaging radiopharmaceutical distributions in nuclear medicine, the tradeoff between system sensitivity and resolution leaves room for improvement in both parameters. There is considerable interest and value therefore in methods of quantitatively characterizing the effects on either of these parameters due to design variations in a system. The ability to measure these effects would permit a gain in either parameter to be exploited if its effect on performance is not offset by associated losses in the other parameter. There is particular interest in methods of characterizing the resolution of a system because of its impact on diagnostic performance through the fidelity of the final image.

Several definitions have been introduced to describe the spatial-resolution characteristics of scanning systems. Although each of these definitions has merit, none has been completely adequate as a description of scanning-system spatial-resolution performance. One of the most commonly used simple indices of spatial resolution, the full width at half maximum (fwhm), is defined as twice the distance a line or point source must be moved from the central axis of the collimator in a plane  $z$  units beneath the collimator face to decrease the counting rate to one half of the value measured on the central axis.

One characteristic of the fwhm is that it does not adequately describe effects important in the wings of the spatial-response function. For example, as one moves the source away from the collimator's central axis, the area of the detector viewing the source is decreased until finally the source is outside the geometric field of view at which time the response falls to zero. However, if septal penetration or scattering within the source or collimator occurs, some response will be observed even after the source has left the field of view. This will cause the response curve to be somewhat broadened and to have a "tail." The extent of broadening and the length of

the tail will be a measure of the system's loss of spatial resolution. Since such broadening of the spread function occurs primarily below the half maximum point, the effects of scattered radiation or septal penetration are not reflected significantly in the fwhm.

Figure 1 shows line-spread functions for a collimator-detector measured in air and in scatter medium for the radionuclide  $^{197}\text{Hg}$ . The energies of  $^{197}\text{Hg}$  (67–78 keV) are low enough that septal penetration in the collimator used is negligible, and therefore the broadening and tail of the spread function are due to scattering only. It will be noted that the fwhm is essentially the same for both curves. Therefore the fwhm is too simple to describe fully the ability of the detection system to respond to fine detail in the presence of appreciable scattering. Penetration of the collimator introduces similar effects with high-energy gamma-ray labels.

Received Jan. 23, 1969; revision accepted Aug. 12, 1969.

For reprints contact: A. G. Schulz, The Johns Hopkins University Applied Physics Laboratory, 8621 Georgia Ave., Silver Spring, Maryland 20910.

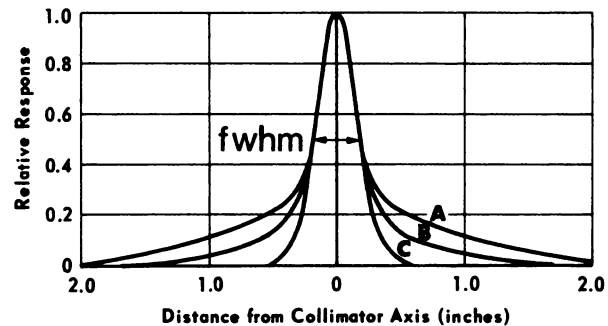


**FIG. 1.** Plot of line-spread function for  $^{197}\text{Hg}$  measured with energy window of 65–100 keV. Response is shown as function of distance from collimator axis for three scatter conditions: Curve A, air; Curve B, 4 in. of backscatter and  $\frac{1}{2}$  in. of frontscatter material (Lucite); Curve C, 4 in. of backscatter and 3 in. of frontscatter material.

Limitations of such simple indices to describe more complex aspects of spatial resolution have caused some authors to turn to the complete response function or its Fourier transform called the modulation transfer function. The modulation transfer function (MTF) was developed to analyze the performance of systems in several other fields. The group at Argonne Laboratory (1-3) and others (4) have recently applied this concept to describe the spatial resolution of scanning. The basic concept relates to the fact that in theory all radiation images may be resolved into a spectrum of spatial frequencies by means of Fourier analysis. The MTF predicts the response of the detection system to the included spatial frequencies.

In the particular task of lesion detection it is generally recognized that the contrast between the lesion area count and the organ background count is a critical parameter. For a sinusoidal test pattern the MTF value at a particular frequency is just the ratio of the image contrast to that of the test object. For a more complex object, such as a lesion in a scan, the effect of the system on contrast may be determined by calculating the spectral function of the image plane (the product of the Fourier transform of the object and the system MTF) and then transforming this function back to a spatial image. In carrying out this latter process, the MTF has special advantages in the analyses of detection systems as pointed out by Morgan (5) and by Gregg (6) since the composite MTF of the entire system may be determined by multiplying the MTF of the component parts, frequency by frequency, across the range of spatial frequencies. This implies that if each component in the image-forming chain can be studied independently of the others, the net behavior of the entire system can be predicted.

The MTF, as discussed so far, provides a curve which predicts the response of the system over a range of spatial frequencies. For determining the precise effect of the system on a well-defined particular input problem, the MTF permits computation of a precise output. The complex calculation provides a spectrum of an output function or, after an inverse transform, a spatial representation of the resultant intensity data. The result does not provide a simple intuitive index of the performance of the system for general classes of inputs or a quantitative index of the change in performance for system changes which vary the MTF curve. For this reason there is still a need for simpler indices which cover generally defined problems and which permit quantitative estimation of the performance as various system parameters are changed.

Among various attempts which have been made to formulate quantitative comparative indices which reflect the overall resolution properties of the system is the use of the area beneath the MTF curve (1). One limitation of this approach is that the index does not weight the frequency response of the system with respect to the frequencies contained in the input problem. When evaluating a system capability for detecting the presence of a ½-in.-dia lesion, the high-frequency response characteristics of the system tend to be of considerably more importance than when the system is used to detect a 1-in.-dia lesion. For example, as may be seen from the data presented later, the frequency response for the frequency range from 1.5 to 3.0 cycles/in. is important for detecting the ½-in. lesion but of less consequence for detecting a 1-in. lesion.

Recently, Gregg (7) has discussed the use of the MTF in a quantitative evaluation of the information capacity of general scanning systems. In this approach, some of the detailed information in the MTF is used along with the width at half maximum to characterize the information capacity per unit area which may be obtained with a given system with a given source intensity. With stated reservations about the usefulness and significance of single figures of merit in discussing complex systems, Gregg indicates that the information capacity per unit area could be used as such a figure of merit within boundary conditions of comparable scan areas and times. This figure of merit does not focus on the particular problem of detecting individual lesions and also does not depend upon the frequency spectrum of the input problem.

With the background of these various indices and functions in mind, a new index called a contrast efficiency function is proposed in this paper. This index takes into account the complete modulation transfer function of the scanning system but will characterize the system on the basis of how this function matches the spectral content of the scanning problem. In the following discussions the contrast efficiency function is defined and applied to the theoretical performance of a series of collimators scanning lesions of graded sizes. It is shown that the new function, computed explicitly from spectral parameters of the scanning system and "lesion," measures the deterioration in contrast resulting from the finite resolution properties of the scanning system. On the basis of experimental measurements with several radionuclides using two collimators and several scatter conditions, the effects of window setting on the contrast efficiency are presented as examples for which losses in resolution show up in the tails of the spatial response function.

## CONTRAST EFFICIENCY

It is adopted here as a basic premise that any index for the characterization of scanning systems should include a dependence on the spectral content of the input problem and how the system-response characteristics match this spectrum. On this basis the use of such an index to make a comparison between two systems or two parametric variations within a system would only be valid for a particular class of problems characterized by similar spectral density functions. An approach which would satisfy this requirement would be to compare the spectrum of an input function (lesion) scanned with a particular system to the spectrum of the same lesion scanned by an ideal system with perfect resolution.

At this point the meaning of what we are calling the spectrum of a lesion must be established. In referring to the spectrum of a scanned lesion, it is assumed that for lesions where detection is a problem the spatial extent of the lesion is small compared with the organ or body and that the spatial distribution of activity of the organ as seen by a scanning system varies slowly compared with that of the distribution of the lesion. If this is true the scan of a lesion leads to a depression or peak in a relatively uniform or slowly varying field of count densities depending on whether we are dealing with a cold lesion in a radioactive organ or a hot lesion in a cold organ. The Fourier transform of the resultant peak (or depression) is what is meant here by the spectrum of the scanned lesion. If the system scanning the lesion has the most ideal resolution which could be obtained with a collimator (two-dimensional resolution only), the resultant image is equivalent to integrating the function which describes the lesion activity,  $A(x,y,z)$ , with respect to  $z$ . The resultant planar distribution function,  $A_1(x,y)$ , would have been obtained from a scan with an ideal collimator whose modulation transfer function is unity out to frequencies beyond those contained in the transform of  $A_1(x,y)$ , at all values of  $z$  in the distribution. We refer to the transform of this function  $A_1(x,y)$  as the spectrum of the lesion alone, designated by  $L(f_x, f_y)$ .

Although the concept presented here is not restricted to cylindrically symmetric lesions or collimator response functions, this discussion will be concerned primarily with such examples. Therefore the spatial variables  $x$  and  $y$  are replaced by the radial distance  $r$ , and the frequency variables  $f_x$  and  $f_y$  are replaced by the radial frequency variable  $f$  in the following sections.

When the lesion is scanned by a real collimator with a modulation transfer function  $M(f)$ , we refer

to the spectrum of the scanned lesion as  $S(f)$  in which

$$S(f) = L(f)M(f). \quad (1)$$

Examples of the spectra of the lesion alone and of a lesion scanned with a collimator with finite resolution are shown in Fig. 2. Curve A, the spectral

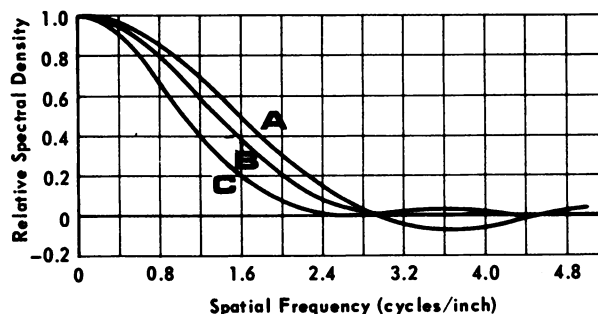


FIG. 2. Relative spectral density functions for  $\frac{1}{2}$ -in.-dia sphere scanned with ideal collimator, Curve A, and with collimator having  $\frac{3}{8}$ -in. radius of view, Curve C. Curve B shows modulation transfer function for collimator-detector system which is compounded with Curve A to generate Curve C.

density function for the lesion alone, and Curve B, the modulation transfer function of the collimator used, are shown. The spectral density function for the scanned lesion is shown in Curve C. The response function of the collimator was run without a scattering medium, and its transform is the modulation transfer function. Whenever a response function is run in a scattering medium, its transform is not the modulation transfer function of the detector system. The transform so obtained is actually a composite modulation transfer function representing the product of an effective modulation transfer function of the scattering medium and that of the detector system. When such a composite MTF is used in this discussion, it will be referred to as  $M_c(f)$ .

Having established the basic variables of the contrast efficiency function, we can now define the function quantitatively and examine its behavior for different problems. Consider the two-dimensional distribution function  $C_s(r)$  describing the cylindrically symmetric spatial distribution function of the scanned lesion defined as follows:

$$\begin{aligned} C_s(r) &= 2\pi \int_0^{\infty} fS(f)J_0(2\pi fr)df \\ &= 2\pi \int_0^{\infty} fL(f)M_c(f)J_0(2\pi fr)df \end{aligned} \quad (2)$$

in which  $f$  is the spatial frequency,  $J_0$  is the zero-order Bessel function of the first kind,  $r$  is the radial distance from the reference origin to the point of

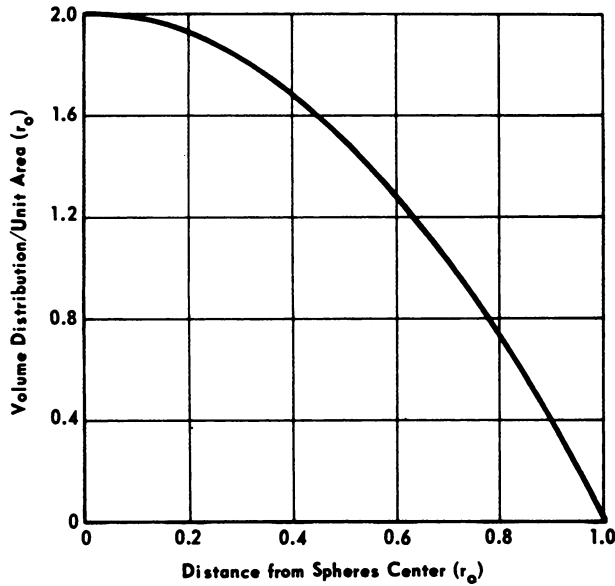


FIG. 3. Projected spatial distribution for sphere of radius  $r_0$  as function of distance from axis of sphere measured in units of  $r_0$ .

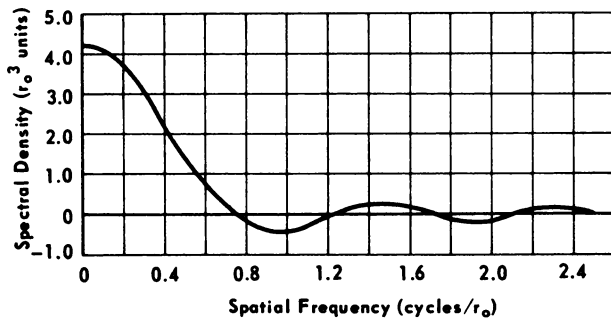


FIG. 4. Spectral density function representing Fourier transformation of projected spatial distribution function for sphere of radius  $r_0$ .

interest and  $S(f)$  is the spectrum of the scanned lesion as defined in Eq. 1. Setting  $r$  equal to zero in the argument of the Bessel function, the amplitude of the distribution at the origin  $C_s(O)$  is obtained:

$$C_s(O) = 2\pi \int_0^\infty fS(f)df. \quad (3)$$

The value of  $C_s(O)$  determines the contrast which would be obtained in a scan with a detector of limited resolution. The actual contrast in the scan is the ratio of the counting rate determined by the lesion activity to that of the background count density in the neighboring regions due to the activity of the rest of the organ and body.

Recalling that the spectral density for a lesion scanned with an ideal system is given by  $L(f)$ , the amplitude of the resultant spatial distribution function  $C_i(r)$  at  $r = 0$  is obtained in a similar manner and found to be

$$C_i(O) = 2\pi \int_0^\infty fL(f)df. \quad (4)$$

The value  $C_i(O)$  determines the contrast which would be obtained in a scan with a detector having ideal resolution. The ratio of the contrast of the scan obtained with finite resolution to the contrast obtained with ideal resolution is the contrast efficiency  $E_c$ .

$$\text{Contrast efficiency} = \frac{\text{Contrast with system of interest}}{\text{Contrast with ideal system}}$$

$$E_c = \frac{C_s(O)}{C_i(O)} = \frac{\int_0^\infty fS(f)df}{\int_0^\infty fL(f)df} = \frac{\int_0^\infty fL(f)M_c(f)df}{\int_0^\infty fL(f)df}. \quad (5)$$

The integrand of the numerator in Eq. 5 is seen to be the first moment of the spectral density function of the lesion scanned with the detector whose modulation transfer function is  $M_c(f)$ . As indicated above, the function  $M_c(f)$  is assumed to correspond to the response in the environment of the lesion. To be of meaning in real scanning problems, all attenuation and scattering effects should be included. The integrand of the denominator is the moment of the spectral density function of the lesion scanned with an ideal collimator. No environmental degradation of resolution is assumed for this function. It is admissible to assume detector response functions measured in air if it is borne in mind that the resultant characterization does not correspond to a real scanning problem. As will be seen in later examples, the combined effects of scattering and attenuation are reflected in the quantitative value of the contrast efficiency function as would be expected from their effects on the form and contrast of the image lesion.

The value of contrast characteristics as a measure of system performance is supported by the recognition of contrast as a fundamental variable in visual perception research. The contrast efficiency provides a simple index of the resolution performance of a system and its effect on the contrast of classes of lesions. The index takes into account the entire spatial response characteristics of the system and yet is fairly simple to compute. The contrast efficiency function characterizes the system with respect to performance in preserving contrast for specified problems or classes of problems with similar spatial resolution characteristics.

THEORETICAL APPLICATIONS

To study the behavior of the contrast efficiency function in a variety of problems covering the range

of typical scanning problems, the contrast efficiency was computed for six collimators for each of three sizes of spherical lesions located in the focal planes of the collimators.

The spectra of the spherical lesions were computed on the basis of the projected volume distribution equivalent to scanning with an ideal collimator as described earlier in this paper. It is noted, however, that length in the spatial domain and frequency in the spectral domain scale in such a way that the projected spatial distribution function and corresponding spectrum computed for one sphere can be scaled to determine the corresponding quantities for a sphere with any other radius. Figure 3 gives the projected volume distribution per unit area for a sphere of radius  $r_0$  as a function of distance from the axis of the sphere. From this figure the spatial distribution function for any size sphere can be generated by substituting the value of its radius. Figure 4 gives the spectral density obtained by performing a Fourier transformation on the spatial distribution function presented in Fig. 3. The units of the abscissa in Fig. 4 are measured in cycles per length  $r_0$ , the radius of the sphere for which the spectrum is to be derived. The spectral density is measured in units of  $r_0^3$ .

To obtain the modulation transfer characteristics for the set of collimators of interest, the point-spread functions of the collimators were calculated theoretically from the response of a single-hole collimator of the focused type. These point-spread functions represent the geometric aperture of the collimator at the focal plane. The Fourier transform of these spread functions are the modulation transfer functions. The modulation transfer functions for four of the collimators with radii of view of  $1/8$ ,  $1/4$ ,  $1/2$  and 1 in. are plotted in Fig. 5. The MTF's for all six of the collimators were used in combination with the three lesion spectral densities to obtain computed contrast efficiencies using Eq. 5. The normalized spectra for the scanned lesion  $S(f)$  in Eq. 1 are presented in Fig. 6 for the  $1/2$ -in. lesion scanned with the collimators having a radius of view of  $1/4$ ,  $1/2$  and 1 in., respectively. The normalized spectrum of the lesion alone, Curve A, is shown for comparison. The  $1/8$ -in. collimator case was not shown since the spectrum differs so little from that for an ideal collimator (lesion alone). The progressive decrease in the high-frequency components of the compound spectra are seen as the resolution of the collimator decreases.

The contrast efficiency function  $E_c$  for the collimators described were calculated for three spherical lesion diameters. The results are plotted in Fig. 7 as a function of the radius of view of the collima-

tors. Examination of Fig. 7 shows that for the simple collimator functions without effects such as scattering and where only the focal plane performance is assumed the contrast efficiency function has equal values for equal ratios of collimator radius of view to lesion size. Even for this simple case some striking features of the degradation of contrast become apparent for increased collimator fields of view. With a typical collimator having a  $3/8$ -in. radius of view,

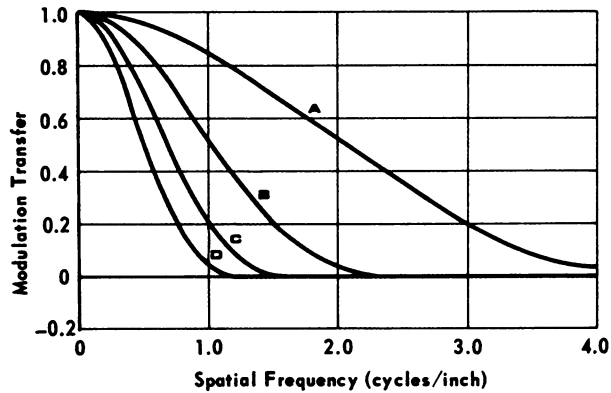


FIG. 5. Modulation transfer functions for collimators with radii of view of (A)  $1/8$  in., (B)  $1/4$  in., (C)  $1/2$  in. and (D) 1 in.

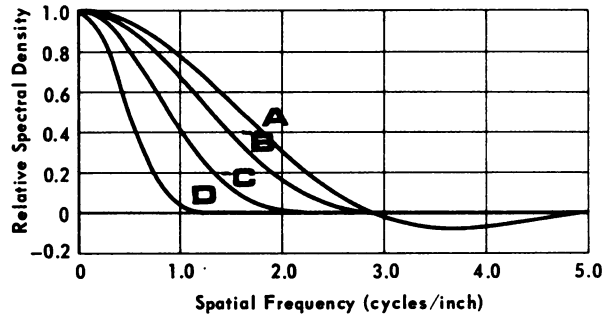


FIG. 6. Normalized spectrum for  $1/2$ -in.-dia spherical lesion scanned with ideal collimator is shown in Curve A. Normalized spectra for scanning same lesion with collimators having radii of view of  $1/4$ ,  $1/2$  and 1 in. are shown in Curves B, C and D, respectively.

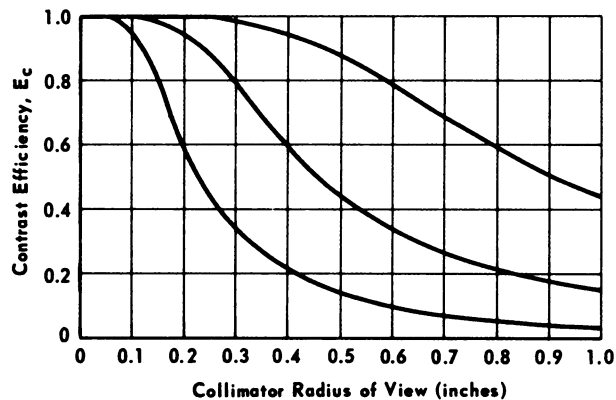
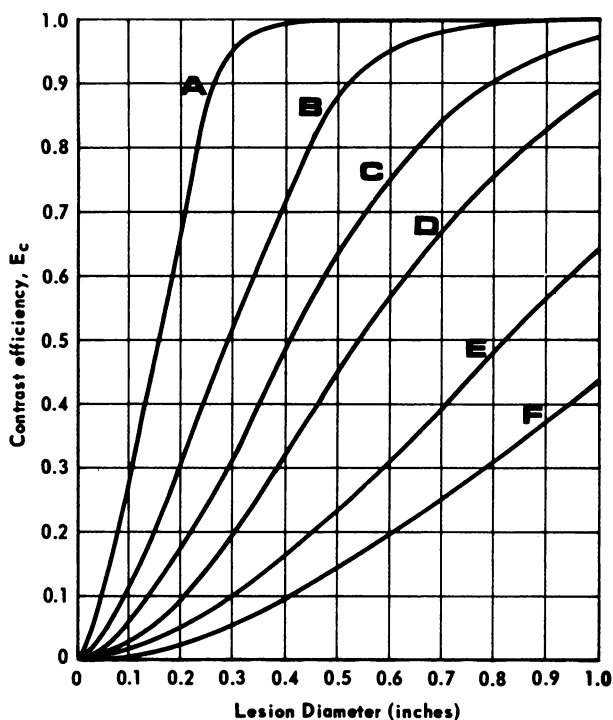


FIG. 7. Upper curve for contrast efficiency is 1-in. lesion, middle curve is  $1/2$ -in. lesion and lower curve is  $1/4$ -in. lesion.



**FIG. 8.** Computed contrast efficiency plotted as function of lesion diameter for collimators having radii of view of  $\frac{1}{8}$  in., Curve A;  $\frac{1}{4}$  in., Curve B;  $\frac{3}{8}$  in., Curve C;  $\frac{1}{2}$  in., Curve D;  $\frac{3}{4}$  in., Curve E; and 1 in., Curve F.

the ideal contrast for a 1-in. lesion is almost completely preserved (95%). For a  $\frac{1}{2}$ -in. lesion with this collimator, the contrast obtained is only about 65% of that which would be obtained with a collimator with very high resolution. It is important at this point to note that the contrast obtained for the  $\frac{1}{2}$ -in. lesion with an ideal collimator is already down to one-half of the contrast of the 1-in. lesion with an ideal collimator from purely geometric considerations. Consequently, the resultant contrast of the  $\frac{1}{2}$ -in. lesion (as it might be presented to a clinician) is really only one-third ( $\frac{1}{2} \times 0.65$ ) of the contrast of the 1-in. lesion when both are scanned with the  $\frac{3}{8}$ -in. collimator. The corresponding relative decrease in contrast for the  $\frac{1}{4}$ -in. lesion with the same  $\frac{3}{8}$ -in. collimator results in approximately one-sixteenth of the contrast obtained with the 1-in. lesion.

Some additional features of the behavior of contrast efficiency as a function of lesion size and collimator radius of view may be observed in Fig. 8. This figure shows contrast efficiency plotted as a function of lesion diameter for several values of collimator radius of view. The curves show how  $E_c$  varies, for example, for the case of a  $\frac{1}{2}$ -in. lesion. The contrast drops from 100%, the ideal value obtained with a  $\frac{1}{8}$ -in. collimator, to 88% for a  $\frac{1}{4}$ -in. collimator, and to 44% and 14%, respectively, for

a  $\frac{1}{2}$ -in. and a 1-in. collimator. It can be seen from the figure that as the lesion diameter approaches zero and the corresponding spectral density function includes increasingly higher frequencies the contrast efficiency function goes to zero. At the other end of the scale, for lesion diameters large compared with the collimator radius of view (approximately four times) the sigmoid curve for the contrast efficiency approaches unity.

EXPERIMENTAL APPLICATIONS

The behavior of the contrast efficiency function was studied experimentally for real detector systems and for cases where scattering significantly affects resolution characteristics. The point-spread functions associated with a Picker Magnascanner II unit were accurately measured for the radionuclides  $^{197}\text{Hg}$ ,  $^{99\text{m}}\text{Tc}$  and  $^{131}\text{I}$  under various scatter conditions for a wide range of lower discriminator pulse-height (gamma-energy) selector settings. The two collimators used have a focal depth of 3 in. Collimator A, used for  $^{197}\text{Hg}$  and  $^{99\text{m}}\text{Tc}$ , had a design resolution of 0.25 in. fwhm, and Collimator B, used with the  $^{131}\text{I}$ , had a 0.50-in. fwhm. The scatter conditions used were air, 4 in. of Lucite backscatter material, 1.5 in. of frontscatter material, 4 in. of backscatter material and 3 in. of frontscatter material.

From the data, the contrast efficiency  $E_c$  for three spherical lesions with different diameters was computed. The variation of  $E_c$  with the lower level

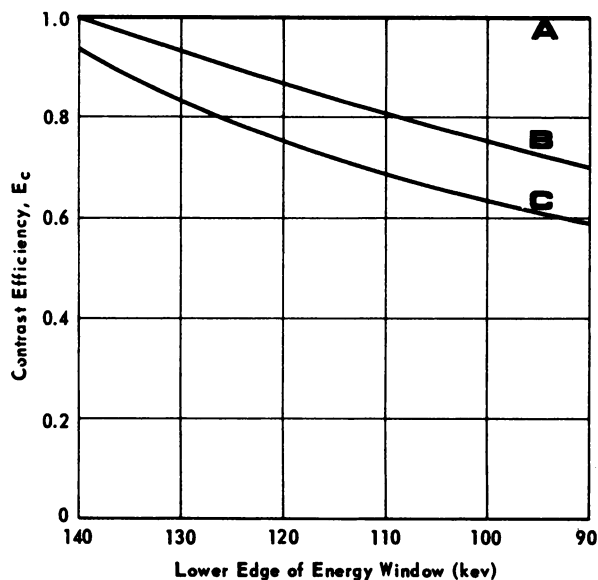


**FIG. 9.** Contrast efficiency for 1-in.-dia spherical lesion as function of value of lower edge of energy window using  $^{99\text{m}}\text{Tc}$ . Upper edge of energy window is 170 keV. Curve A is performance in air. Curves B and C are for performance with 4 in. of Lucite backscatter material and for  $1\frac{1}{2}$  in. and 3 in. of frontscattering material, respectively. Collimator used (Collimator A) has 3-in. focal depth and  $\frac{1}{4}$  in. fwhm.

energy discriminator window setting for the radionuclide  $^{99m}\text{Tc}$  and for a 1-in. lesion under the three scatter conditions are presented in Fig. 9. It can be seen from Fig. 8 that the theoretical  $E_c$  for a 1-in.-dia lesion and a 0.25-in. radius-of-view collimator is unity. It is not surprising therefore that the  $E_c$  for the 0.25-in. fwhm collimator used in air, Curve A of Fig. 9, is equal to unity and shows no decrease with changes in energy-window baseline setting. The fact that this contrast efficiency measured in air is independent of the window setting results from the fact that no significant scattering effects are occurring to provide lower energy photons.

The curve for  $E_c$  measured for  $^{99m}\text{Tc}$  with scattering material present, Curves B and C of Fig. 9, show little change in  $E_c$  when the lower edge of the energy window is as high as the center of the photopeak. For the technetium gamma energy this setting discriminates against photons scattered through appreciable angles. As the energy window is lowered, the angular aperture through which the detected photons may be scattered is increased and the contribution of these photons causes a steady, nearly linear decrease in the contrast efficiency.

Contrast efficiencies for each of the three radionuclides are plotted in Fig. 10 as a function of lesion diameter for air conditions using the collimators described earlier. The energy window for  $^{197}\text{Hg}$  was 55–100 keV, for  $^{99m}\text{Tc}$ , 130–170 keV, and for  $^{131}\text{I}$ , 325–405 keV.\* These experimental results are consistent with the theoretical  $E_c$ -versus-lesion-diameter curves presented in Fig. 8. The curves in Fig. 8 are not exactly comparable to the curves of Fig. 10 because the collimator resolution characteristics are specified in terms of the radius of view in Fig. 8 and in terms of fwhm in Fig. 10. A collimator of specified fwhm has a slightly larger radius of view. Although the same collimator was used for both the  $^{99m}\text{Tc}$  and  $^{197}\text{Hg}$  measurements, the  $^{99m}\text{Tc}$  efficiency is higher than the  $E_c$  for  $^{197}\text{Hg}$ . The only scatter contributions in this case are the forward scattered photons from the walls of the lead collimator. The  $^{197}\text{Hg}$  photons scattered off the collimator walls lose little or no energy per scattering event and are accepted by the detector discriminator. At the  $^{99m}\text{Tc}$  photon energies the energy losses tend to remove the scattered photons from the energy acceptance level of the window. The corresponding degradation in resolution characteristics with  $^{197}\text{Hg}$  are reflected in the lower contrast efficiency.

In Fig. 11 the contrast efficiency is plotted as a function of lesion diameter for the three radionu-

\* It was correctly pointed out by the reviewer that the selection of the 55–100-keV energy window for  $^{197}\text{Hg}$  was not optimum with respect to preserving contrast.

clides of interest for measurements made with 4 in. of backscatter material and 3 in. of frontscatter medium, a condition of interest in typical scanning problems. The  $^{131}\text{I}$  curve is similar to the  $^{131}\text{I}$  air curve shown in Fig. 10. This is due to the fact that photons of  $^{131}\text{I}$  scattered at any finite angle lose enough energy to place them outside the photon energy range being passed by the detector energy discriminator. Figure 11 shows the  $E_c$  for collimator A run with  $^{99m}\text{Tc}$  to be higher by a factor of two than that obtained for  $^{197}\text{Hg}$ . This drastic and perhaps unexpected result of scattering indicates that a scan of any lesion in the diameter range considered would provide a factor of two in the contrast. This difference, which will have a strong effect upon the lesion detectability, is independent of counting rate and is a function of the amount of scattering material and the photon energies involved. The manner in which

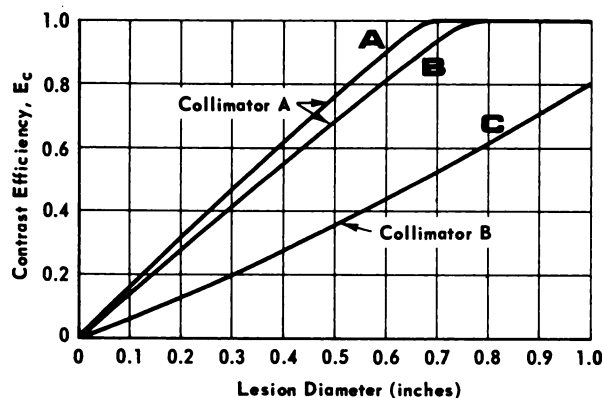


FIG. 10. Contrast efficiencies are plotted as function of lesion diameter for response functions experimentally measured in air with Collimator A (0.25-in. fwhm) using  $^{99m}\text{Tc}$  (Curve A) and  $^{197}\text{Hg}$  (Curve B) and with Collimator B (0.5-in. fwhm) using  $^{131}\text{I}$  (Curve C). Energy acceptance windows were 55–100 keV for  $^{197}\text{Hg}$ , 130–170 keV for  $^{99m}\text{Tc}$  and 325–405 keV for  $^{131}\text{I}$ .

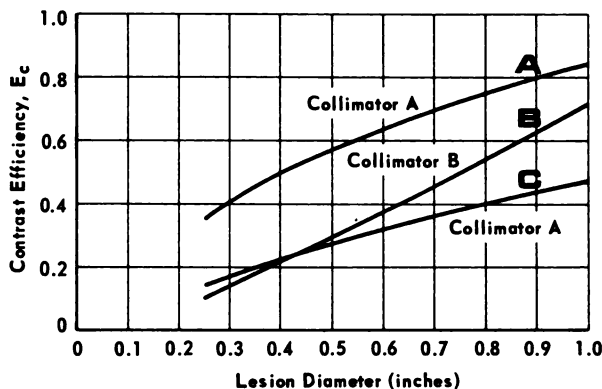
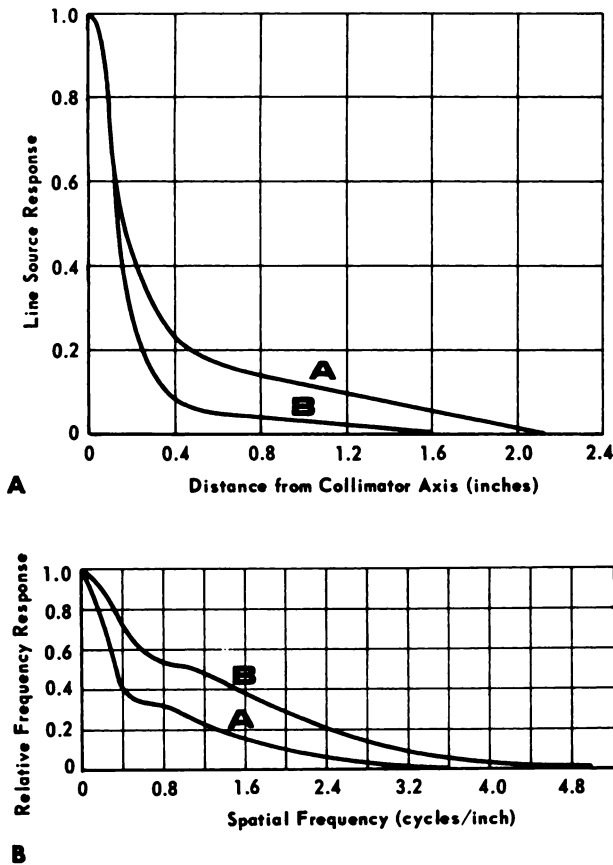


FIG. 11. Contrast efficiencies are plotted as function of lesion diameter for response functions experimentally measured with 4 in. of Lucite backscatter material and 3 in. of Lucite frontscatter material. Collimators and window settings are those given in Fig. 10. Curves A and C are for performance of Collimator A with  $^{99m}\text{Tc}$  and  $^{197}\text{Hg}$ , respectively. Curve B is for the performance of Collimator B with  $^{131}\text{I}$ .



**FIG. 12.** A shows line-spread functions for  $^{197}\text{Hg}$  (Curve A) and for  $^{99\text{m}}\text{Tc}$  (Curve B) run with Collimator A (0.25-in. fwhm) for scattering configuration with 4 in. of Lucite backscatter and 3 in. of Lucite frontscatter material. Energy windows are 55–100 keV for  $^{197}\text{Hg}$  and 130–170 keV for  $^{99\text{m}}\text{Tc}$ . B is corresponding composite modulation transfer functions for Collimator A with  $^{197}\text{Hg}$  (Curve A) and with  $^{99\text{m}}\text{Tc}$  (Curve B).

these results are reflected in the measured line-spread functions is shown in Fig. 12A. The corresponding modulation transfer functions computed from the measured line-spread functions using the equation of R. Clark Jones (8) are shown in Fig. 12B.

These results further demonstrate the applicability of the contrast efficiency concept for evaluating variations in spatial-resolution performance as scanning-system parameters are changed.

**CONCLUSION**

A new function is proposed to fulfill a standing need for a quantitative method for characterizing the resolution of a scanning system. It is postulated that

any characterization of the resolution of a system must be referred to an input problem or related class of problems. To provide a definition for the input problem, the concept of the spectrum of a lesion or organ is proposed and defined on the basis of the transform of the representation of a scan made with an ideal system. The contrast efficiency function is then defined as the ratio of the contrast obtained in a scan of a lesion with a system of interest to that obtained with such an ideal system.

Mathematically, the function is a measure of how well the transfer function of the system matches the spectral density of the scanning problem. The  $E_c$  concept has special advantage since it permits comparison of resolution performance between systems as well as within a single system where parameters affecting resolution characteristics are varied.

**ACKNOWLEDGMENTS**

The authors wish to express their thanks to L. C. Kohlenstein for his valuable suggestions regarding the interpretation of the contrast efficiency function. This work was aided by U.S. Public Health Service Grant GM 10548 and Radiological Health Training Grant 39896-03-68.

**REFERENCES**

1. BECK, R. N., HARPER, P. V., CHARLESTON, D. B. AND YASILLO, N. J.: Improvement of image quality of photo-scans by spatial filtering. *J. Nucl. Med.* 8:286, 1967.
2. HARPER, P. V., COHEN, T. D. AND BECK, R. N.: An information transfer function for evaluation of scanning procedures. *J. Nucl. Med.* 8:283, 1967.
3. GOTTSCHALK, A., COHEN, T. AND BECK, R. N.: Optimization of spectrum analysis for pancreas and parathyroid scanning with selenium-75. *J. Nucl. Med.* 8:321, 1967.
4. CRADDOCK, T. O., FEDORUK, S. O. AND REID, W. B.: A new method of assessing the performance of scintillation cameras and scanners. *Phys. Med. Biol.* 11:423, 1966.
5. MORGAN, R. H.: Visual perception in fluoroscopy and radiography. *Radiology* 86:402, 1966.
6. GREGG, E. C.: A pedagogical note on modulation transfer function. *Inv. Radiol.* 6:418, 1966.
7. GREGG, E. C.: Modulation transfer function, information capacity and performance criteria of scintiscans. *J. Nucl. Med.* 9:116, 1968.
8. JONES, R. C.: On the point and line spread functions of photographic images. *J. Opt. Soc. Am.* 48:934, 1958.